Provincial Scale Monitoring of Mangrove Area and Smooth Cordgrass Evasion in Subtropical China Using UAV Imagery and Machine-Learning Methods

Qiliang Lv , Peng Zhou , Sheng Yang , Yongjun Shi , Jiangming Ma , Jiangcheng Yang , Guangsheng Chen *

Posted Date: 11 December 2025

doi: 10.20944/preprints202512.0901.v1

Keywords: Unmanned Aerial Vehicle (UAV) imagery; mangrove forest; smooth cordgrass (*Spartina alterniflora*); invasive species; machine learning method

Article

Provincial Scale Monitoring of Mangrove Area and Smooth Cordgrass Evasion in Subtropical China Using UAV Imagery and Machine-Learning Methods

Qiliang Lv [1,2], Peng Zhou [1,2], Sheng Yang [3], Yongjun Shi [1,2], Jiangming Ma [4], Jiangcheng Yang [1,2] and Guangsheng Chen [1,2,*]

[1] College of Environment and Resources, College of Carbon Neutrality, Zhejiang A&F University, Hangzhou 311300, China

[2] Key Laboratory of Carbon Sequestration and Emission Reduction in Agriculture and Forestry of Zhejiang Province, Hangzhou 311300, China

[3] Zhejiang Institute of Subtropical Crops, Zhejiang Academy of Agricultural Sciences, Wenzhou, 325005, China

[4] Key Laboratory of Ecology of Rare and Endangered Species and Environmental Protection, Ministry of Education, Guangxi Normal University, Guilin 541006, China

* Correspondence: chengu1@zafu.edu.cn

Highlights

1. The canopy coverage area for mangrove trees and smooth cordgrass was 140.83 and 52.96 ha in Zhejiang Province.
2. The survival rate of mangrove trees was 36.41% while the invasion rate of smooth cordgrass was 13.70%.
3. Smooth cordgrass invasion rates in some districts were higher than 67.3%, suggesting active control and replanting of mangrove trees are needed.
4. Smooth cordgrass invasion can be suppressed when mangrove canopy coverage is greater than 40%.

Abstract

The survival and growth of mangrove along the coastal China was threatened by the invasive smooth cordgrass (*Spartina alterniflora*). Due to the high mortality and frequent replanting of mangrove trees and impacts of invasive smooth cordgrass, it is still unclear about the exact mangrove forest area in Zhejiang Province, China. Based on provincial scale UAV imagery and large numbers of field survey plots, this study classified the area and distribution of mangroves and the invasion status of smooth cordgrass using the identified machine-learning method. The accuracy assessment indicated that the overall accuracy and Kappa coefficient were 97% and 0.96, respectively for land cover classifications. The total area of mangrove forest and smooth cordgrass was 140.83 ha and 52.95 ha, respectively in Zhejiang Province. The mangrove forest area was mostly concentrated in Yuhuan, Dongtou, Yueqing and Longgang districts. The overall survival rate of mangrove trees was only 36.41%, with lower than 20% survival rates in all northern and some central districts. At spatial scale, the mangrove trees showed a scattered distribution pattern, and over 70.04% of the planting area has canopy coverage lower than 20%, indicating a high mortality rate. Smooth cordgrass has widely invaded in all 11 districts, accounting for about 13.7% of the total planting area of mangrove trees. Over 67.3% and 85.4% of the planting area has been occupied by smooth cordgrass in Wenling and Jiaoxiang districts, respectively, which calls for an intensive anthropogenic intervention to control the spreading of smooth cordgrass in these districts. Our study provides a more accurate monitoring of the mangrove and smooth cordgrass distribution area at a provincial scale. The findings will help guide the replanting and management activities of mangrove trees and the control planning of smooth

 doi:10.20944/preprints202512.0901.v1

cordgrass, and also provide data basis for accurate estimation of carbon stock for mangrove forests in Zhejiang Province.

Keywords: unmanned aerial vehicle (UAV) imagery; mangrove forest; smooth cordgrass (*Spartina alterniflora*); invasive species; machine learning method

1. Introduction

Mangrove ecosystems are tidal flat wetland woody plant communities comprising mainly tree and shrub plants in the tropical and subtropical regions[1]. Mangroves are critical ecosystems, bridging land, freshwater and sea, and play a pivotal role in the coastal social, ecological, economic, and other ecosystem services[2,3]. There were 147,359 km^2 of mangrove forests distributed worldwide in 2020, with an area loss of 3.4% during 1996-2020[3]. During 2000-2016, over 62% of global mangrove forests were lost primarily due to direct and indirect human impacts[4]. Similarly, approximately 62% of China's mangrove forests were lost between 1973 and 2000[5,6]. The continued decline of mangrove forests is generally caused by conversion to agriculture, aquaculture, tourism, urban development and overexploitation[1]. However, invasive species can also threaten the persistence of mangrove forests[7]. Smooth cordgrass (*Spartina alterniflora*) is one of the most successful invasive species in mangrove wetlands and has dispersed coast-wide to all mangrove sites in China[8], underscoring the need for the integration of invasive plant management strategy into mangrove forest management[9]. Smooth cordgrass was first introduced to China in 1979. Since then, this species has proliferated along the coast of China, spreading from the southern tropical (i.e., Hainan Province) to the northeastern temperate (i.e., Liaoning Province) coastlines[10]. In 2003, the smooth cordgrass was recognized as an invasive species in China by the Ministry of Ecology and Environment. Characterized by high adaptability and rapid reproduction, smooth cordgrass can proliferate over large areas after invasion, thereby encroaching on the habitats of mangroves and affect the ecosystem stability[11,12]. However, the role of the invasion of smooth cordgrass to the degradation of mangrove forests has received little attention[9,13].

Zhejiang Province is the most northern boundary suitable for mangrove forests in China[14]. Due to the limitation of air temperature, the main mangrove species of *Kandelia obovata* is artificially cultivated and planted in this province. This tree species can grow up to 6 m in the tropical region of China, but in Zhejiang Province, the tree height of mature *K. obovata* forests is declined from about 3 m in the southern coast to lower than 1 m in the northern coast[15]. All mangrove forests in this province were artificially planted. The suitable habitats of mangrove trees are overlapped with smooth cordgrass, and most mangrove trees were planted after the smooth cordgrass was mechanically removed[16,17]. Due to the lower height and slow growth rates and less competitive for *K. obovata*, the smooth cordgrass can easily reinvade into the mangrove forests. The invasion of smooth cordgrass can either cause the death of mangrove trees or poor growth due to resource competition or overshadow. In addition, the high density and extensive root system of smooth cordgrass create a "green desert" in its distribution areas, which poses a significant threat to intertidal biodiversity[8,18]. The local government is striving to recover the mangrove forests and remove the invasive smooth cordgrass. The Special Action Plan for Mangrove Conservation and Restoration (2020–2025) was issued in 2020 and under this plan, Zhejiang Province plans to afforest 690 ha mangrove forests, accounting for 182% of current area (385 ha)[15]. To help identify the suitable planting area and mitigate the impacts from smooth cordgrass, accurate monitoring of present mangrove and smooth cordgrass distribution area and landscape patterns is urgently needed.

Due to the advantages with larger spatial coverage, less cost, and various scales and resolution, remote sensing tools have been widely applied to detect the invasion of smooth cordgrass into mangrove forests in the past decades[7,12,13,19]. Based on the Landsat imagery, Wu et al. [17] monitored the dynamic changes of smooth cordgrass and mangrove area and landscape patterns from 2005 to 2021 in the Zhangjiang Estuary, Zhejiang Province. Based on Gaofen-1 multispectral

 doi:10.20944/preprints202512.0901.v1

imagery, Li et al.[16] monitored and assessed the spreading of smooth cordgrass in the mangrove forests at Shankou Mangrove Reserve, Guangxi Province. These satellite platforms were successfully applied to monitor the spatiotemporal change patterns of smooth cordgrass and mangrove forests at regional, national or global scales; however, these platforms are not suitable and accurate enough for detecting the dynamic changes of these two vegetation types in the area with scattered distribution and short plants. For example, the detected area of mangrove forests in Zhejiang varied from 6.12 ha to 386.77 ha based on the classifications from different satellite platforms such as Landsat, SPOT, Sentinel-2, ALOS, WorldView and Gaofen-1[3,5,14,20,21], implying a large uncertainty in the estimated mangrove forest area in Zhejiang Province, mainly due to the compounding effects from the smooth cordgrass[20,21]. A few satellite-based studies have also reported the smooth cordgrass invasion into mangrove forests[12,22,23]. Liu et al.[24] applied multi-sources of high-resolution satellite images to monitor the invasion of smooth cordgrass into the mangrove forests. In recent years, a few studies begun to apply UAV imagery to detect the invasion of smooth cordgrass into mangrove forests[12,13,23]. For example, Kan et al. [13] applied the UAV images and machine learning methods detected the coverage for both smooth cordgrass and mangrove trees in an estuary of Fujian Province and achieved excellent performance, suggesting the UAV method can be more accurate applied especially at plot and ecosystem scales. However, few studies have been conducted to detect coverage of both mangrove trees and smooth cordgrass at provincial scale.

Based on the single-date provincial level UAV imagery, our study aims to detect the coverage of both mangrove trees and smooth cordgrass and assess the invasion status of smooth cordgrass into mangrove forests. More specifically, our study seeks to address three research questions: (1) Which classification method is the most suitable for detection of both mangrove trees and smooth cordgrass based on the UAV imagery? (2) How much mangrove trees are actually survived and where they are located? (3) What is the invasive status of smooth cordgrass and the implications for management in Zhejiang Province? The findings will help guide the conservation and planting planning of mangrove trees, and the scientific control of smooth cordgrass invasions in Zhejiang Province.

2. Materials and Methods

2.1. Study Area

The study area is located at the coastline of Zhejiang Province (27°03′–31°04′N, 119°37′–123°25′E) (Figure 1). The study region is characterized by a middle-to-northern subtropical maritime monsoon climate. The annual average temperature is 17.7 °C, the annual average rainfall is 1507 mm, and the frost-free period is 258 days. All mangrove forests in this province are artificially planted. Based on the previous inventory and the governmental statistical documents, only several cities or districts have planted mangrove trees, including the cities of Zhoushan, Taizhou, and Wenzhou. The mangrove forests are often threatened by the extreme low temperature in this region. The field experiments indicated that the lower limit temperature for mangrove forests is -5°C, so the most northern distribution area is the Zhoushan City[15,25]. The majority (>95%) of the mangrove species is K. obovata. *K. obovata* is an evergreen mangrove tree species belonging to the *Rhizophoraceae* family and *Kandelia* genus. The highest height of this species is about 6 m in China. This species is first introduced from Fujian Province, China and was cultivated using the tissue culture method to make them suitable for growth in Zhejiang Province[25]. Except for the mudflat area at the leeward bay, all distribution area of smooth cordgrass is also suitable for *K. obovata* too[24].

Most of the mangrove trees were planted in the smooth cordgrass distribution area after the smooth cordgrass is mechanically removed. The smooth cordgrass was first introduced to Zhejiang in 1983 and expanded thereafter to 5,092 ha based on inventory data[11]. This invasive species poses a serious threat to mangroves through stronger competition due to its ecological niche overlap with mangrove species especially in the northern limits of mangrove distribution in Zhejiang Province, where the mangrove trees grow slower than smooth cordgrass. In addition, the height of smooth

 doi:10.20944/preprints202512.0901.v1

cordgrass is often higher than that of mangrove trees in Zhejiang Province, also causing overshadow condition and tree mortality.

Due to the mangrove area is relatively small and scattered widely, we divided the distribution areas into 11 districts for analysis and mapping convenience, including Putuo, Sanmen, Jiaojiang, Wenling, Yueqing, Yuhuan, Dongtou, Rui'an, Pingyang, Longgang and Cangnan districts (Figure 1).

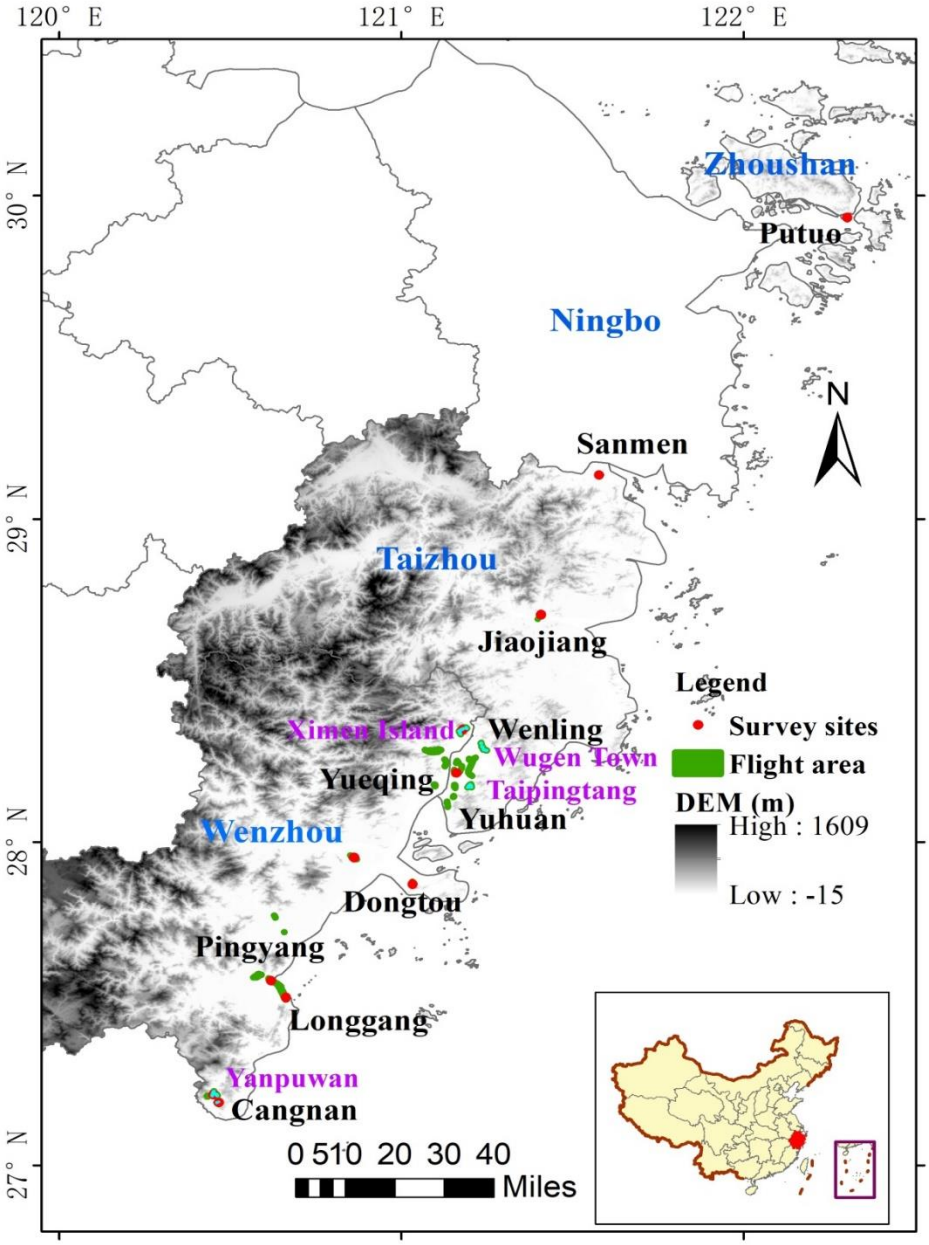

Figure 1. The study area with mangrove forest distribution (Blue city names), 11 field survey sites (Red points), UAV flight areas (Green polygons), test regions (Pink polygons and names) and the divisions of 11 analysis areas (Black names).

2.2. The Work Flow

The work flow of our study method consisted of various phases, as shown in Figure 2. More detailed descriptions for the work flow were shown below.

 doi:10.20944/preprints202512.0901.v1

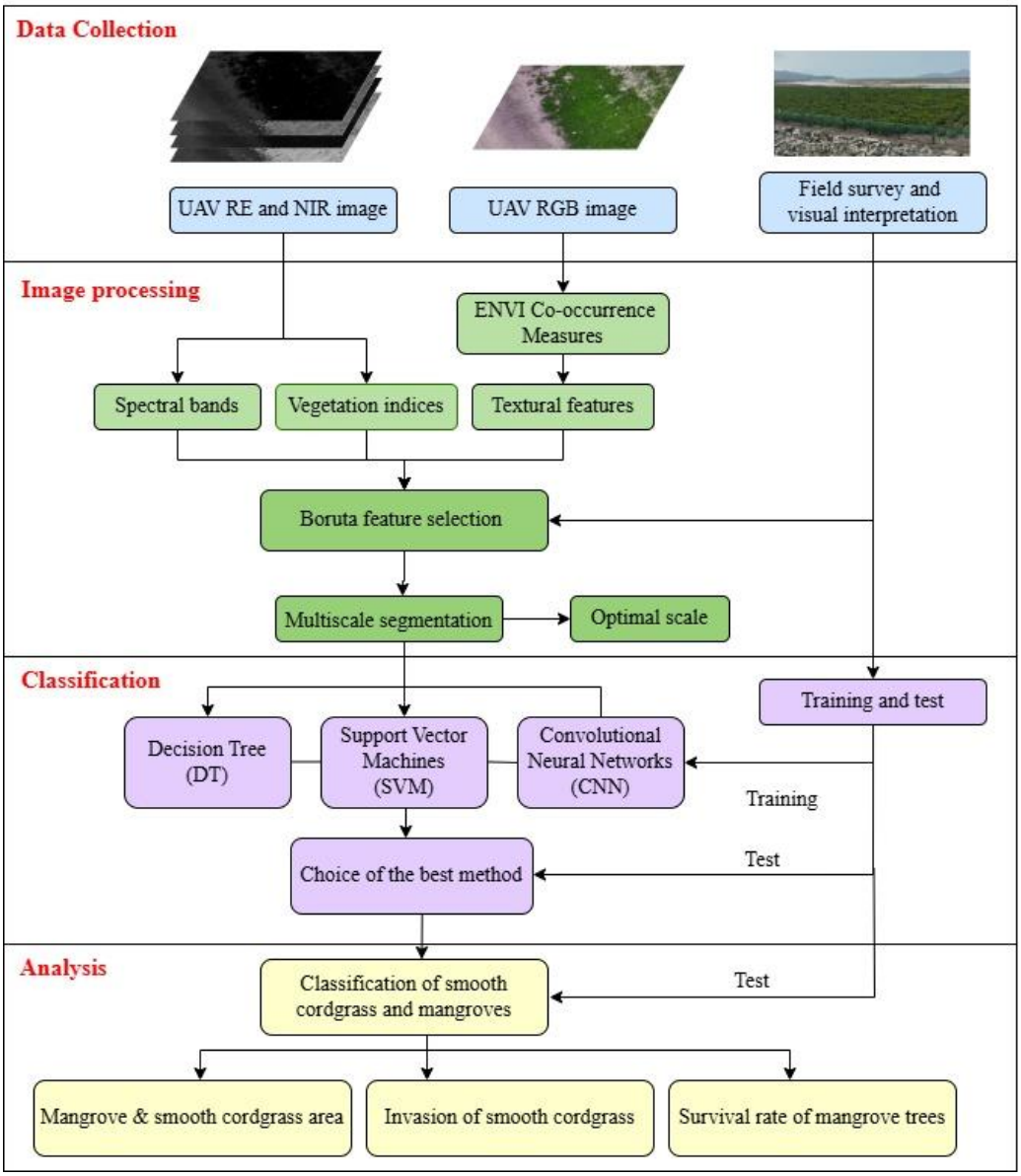

Figure 2. The work flow of this study.

2.3. UAV Image Collection

The multispectral airborne images were collected during the low tide period on August 8-15, 2023, using a DJI MAVIC 3 PRO UAV. The regions of interest for flights were first determined based on the inventory planting area boundary (Figure 1). The flight route was designed and planned by DJI Fly, with an 80% flight overlap and 75% lateral overlap. The exposure time was 1/640s, the ISO speed was 100, and the flight altitude was 100 meters. The UAV is equipped with a multispectral camera, a global navigation satellite system (GNSS), and real-time kinematic (RTK) instrument. The multispectral sensor has five bands: green (G), red (R), Blue (B), red edge (RE), and Near-Infrared (NIR). The UAV is equipped with a light intensity sensor that is capable of automatically adapting to ambient light conditions, thereby facilitating the acquisition of enhanced NDVI data during reconstruction. The weather conditions during the data collection were very suitable for flight, with low wind velocity. The UAV images for different levels of evasion were shown in Figure 3.

 doi:10.20944/preprints202512.0901.v1

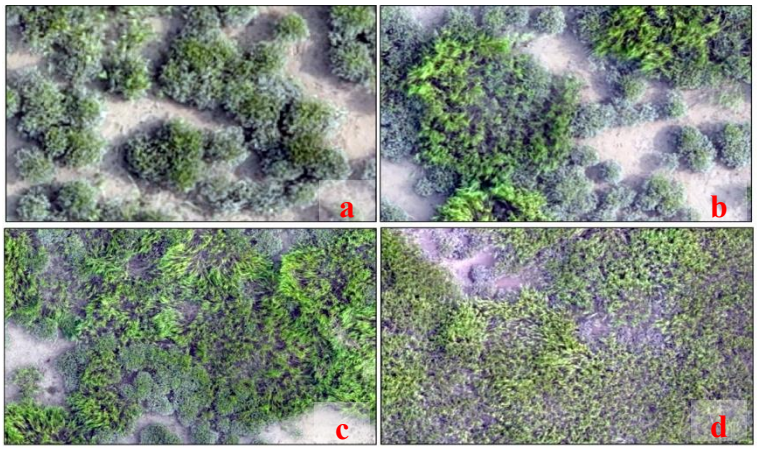

Figure 3. The UAV images for different invasive rates of mangrove forests (a: 100% mangrove trees; b: 60% mangrove trees; c: 30% mangrove trees; d: 100% cordgrass).

2.4. Ground-Truth Survey and Sampling Data Collection

A full field inventory was conducted during August 23-29, 2023 along the coastal line of Zhejiang Province from the south (Wenzhou City) to the north (Zhousan City). The plot coordinates and sampling point locations were recorded using the survey-grade GPS receivers of Huace RTK (Everest Edition), with 8 mm horizontal accuracy and 15 mm elevation accuracy. Due to the difficulty to separate individual mangrove tree canopy and lower height, we set up each 5×5 m plot to represent the plot-scale average conditions. For mangrove trees, the investigated variables include average and maximum tree height, mean canopy coverage (percent of land area), mean basal diameter, and tree numbers within each a plot. For smooth cordgrass, the mean height and coverage within a plot was investigated. The fraction of canopy coverage by mangrove trees and smooth cordgrass in each plot was then manually calculated. In addition, to increase sampling size, we also conducted visual interpretation to calculate the canopy coverage for all land cover types. Totally, 1534 sampling plots were collected, including 251 plots for mudflat, 149 plots for water body, 139 plots for built-up land, 479 plots for mangrove trees, 362 plots for smooth cordgrass, and 154 plots for others (Figure 1).

2.5. Image Processing

The image preprocessing was conducted using the DJI Terra software (DJI, Shenzhen, China), which provides comprehensive image preprocessing steps for DJI UAVs, facilitating the acquisition of data. The flight route was processed and stitched to generate an orthophoto map. The atmospheric correction, radiometric calibration, and reflectance correction were performed to remove the distortion. Finally, the image is cropped as study area according to the reported planted area for mangrove trees.

Previous research has proved that texture features, vegetation indices, and spectral bands can be applied to differentiate mangrove trees and other vegetation types. Therefore, we selected the reflectance values of four bands (R, G, NIR, and Red Edge), four vegetation indices (Normalized Difference Vegetation Index, NDVI; Normalized Difference Red Edge Vegetation Index, NDRE; Green NDVI, GNDVI; and Leaf Area Index, LAI), and texture variables (the mean, variance, homogeneity, contrast, dissimilarity, entropy, second moment, and correlation). The eight texture variables were calculated for each band using the Gray-Level Co-occurrence Matrix (GLCM). The chosen moving window was 7 × 7 pixels.

Table 1. The extract features for classification.

Object Features	Description
Spectral bands	Red (R); Green (G); Red Edge (RE); Near-infrared (NIR)

 doi:10.20944/preprints202512.0901.v1

Vegetation indices	Normalized Difference Red Edge Vegetation Index (NDRE), Normalized Difference Green Vegetation Index (GNDVI), Leaf Area Vegetation Index (LAI), Normalized Difference Vegetation Index (NDVI)
Textural variables	Mean, variance, homogeneity, contrast, dissimilarity, entropy, second moment, correlation

The Boruta algorithm was employed in the screening of the key and most important classification features. The Boruta algorithm is capable of identifying all quantities that exert a significant influence on the classification outcome[26]. The fundamental premise is to statistically ascertain the significance of actual variables and those that have been randomly introduced. Furthermore, it is capable of considering the relationship between multiple variables. The importance of all 33 input variables for the machine-leaning classification of land cover types was ranked. The 10 variables with the highest classification capability were identified based on the feature importance index. As shown in Figure 4, the five most important features were G_correlation, G_mean, R_correlation, B_mean, and GNDVI, indicating the texture features are more important than vegetation indices and spectral bands, especially to differentiate the mangrove trees and smooth cordgrass.

The land cover types were subdivided into five primary categories including nuilt-up land (BU), mangroves (MA), mudflats (MU), smooth cordgrass (SC) and water body (WA).

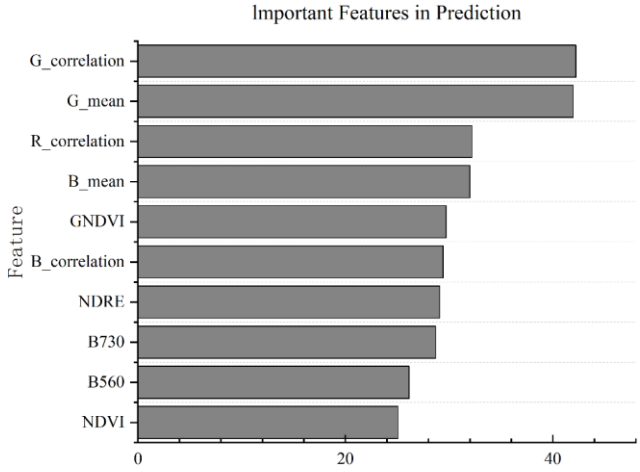

Figure 4. The selected top 10 features and their relative importance.

2.6. Multi-Scale Segmentation

Due to the high spatial resolution and different sizes of varied objects, multi-scale segmentation rather than pixel-based classification method is applied to remove the "salt-and-pepper noise" and increase the feature extraction accuracy[27]. Multi-scale segmentation is a step in the object-oriented classification that divides pixels into discrete units, thereby facilitating the formation of objects comprising pixels with similar characteristics at a given scale. The FbSP (Fuzzy-based Segmentation Parameter) optimizer in eCognition 10.3 software was selected to determine the optimal segmentation parameters including scale, shape/color, and smoothness/compactness. The scale parameter represents the size of the segmentation (the maximum heterogeneity degree of objects), while the shape parameter represents the weight assigned to the segmentation criterion. An elevated compactness index indicates a more compact image [28].

The shape index, compactness and scale parameters were adjusted to perform a series of tests. The ranges for shape index and compactness parameters were set from 0.1 to 0.9, while the scale parameters are set from 10 to 100. The results showed when the scale is set to 70, the neighboring objects with similar features are often misclassified. When the scale was set to 50 or 30, the

 doi:10.20944/preprints202512.0901.v1

segmentation results were too fragile, which affected the efficiency of subsequent image processing (Figure 5A). When the shape index was set as 0.1, 0.3, and 0.7, adjacent objects with some shape similarities were grouped into one category. This included cases such as mangroves and smooth cordgrass (Figure 5B). Visual inspection of the segmentation results showed that when the compactness was 0.5, the objects of each land cover type were more compact and the overall segmentation result was visually most satisfactory (Figure 5C). Accordingly, when evaluating the clustering characteristics of the distribution of mangrove communities in the study area, the optimal scale, shape, and compactness parameters were determined as 70, 0.3, and 0.5, respectively, based on multiple interactive segmentation trials.

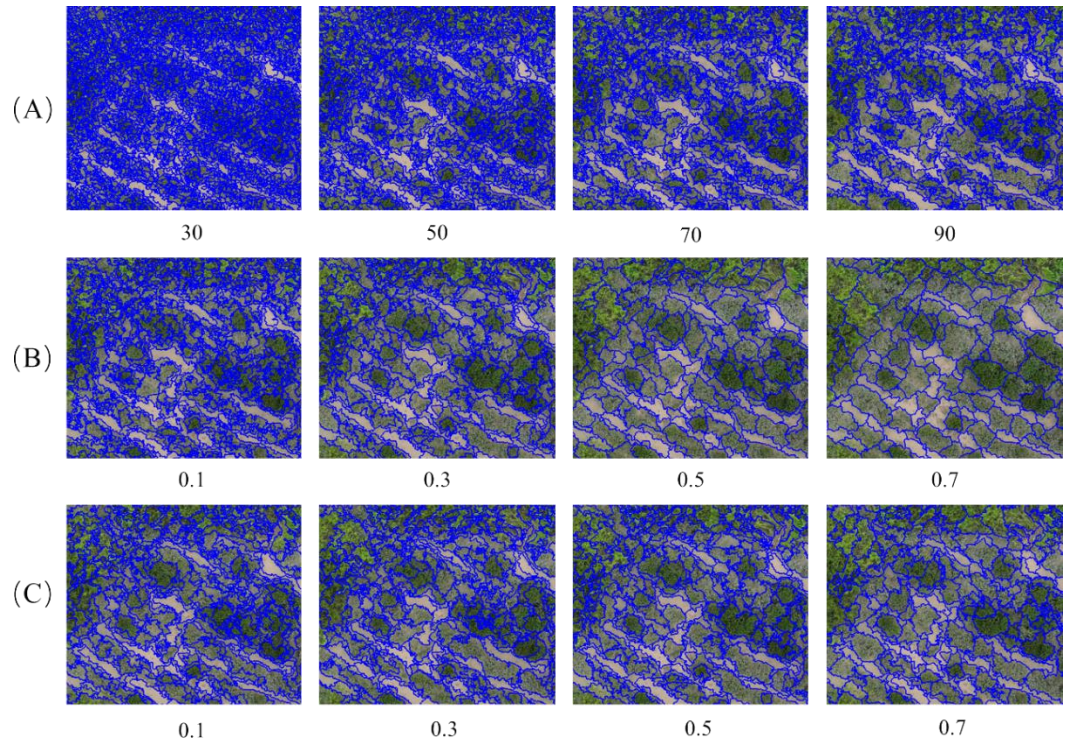

Figure 5. Local representation of the image segmentation for different scale factors, shape indices and compactness parameters. (A) image segmentation results with different scales (shape index = 0.1, compactness = 0.5), (B) image segmentation results with different shape indices (scale = 70, compactness = 0.5), (C) image segmentation results with different compactness values (scale = 70, shape index = 0.3).

2.7. Classification Methods

We applied the object-oriented classification methods to detect land cover types in the study area, which is based on optimal segmentation parameters and the selected features. The most commonly support vector machine (SVM), CART decision tree (DT), and convolutional neural networks (CNN) algorithms are chosen to evaluate their performance. These methods have all been previously applied to detect mangrove and smooth cordgrass[13,29,30].

The SVM is an advanced supervised learning algorithm that can be used as a non-parametric classifier for land cover classification based on multispectral imagery, including the classification of mangrove species. SVM is based on statistical learning theory and aims to identify the optimal decision hyperplane in high-dimensional space, thereby achieving the best possible category separation. In the context of uncertain classification problems with high-dimensional features, SVM has demonstrated consistent performance, even with a limited number of training samples[30].

The decision tree algorithm partitions data into numerous subsets and represents decision rules and classification outcomes in a tree-like data structure, frequently a multi-node tree[31]. CART is a decision tree regression model that can be employed for both classification and regression analysis. CART is mainly applied to land-cover mapping, disaster monitoring, and crop identification. This

 doi:10.20944/preprints202512.0901.v1

algorithm offers several advantages: the rules are transparent and easy to interpret, the tree can be adjusted effortlessly afterwards, and it supports refined multi-class discrimination. Decision trees are split into classification trees and regression trees on the basis of the predictor variables: when the response is discrete the tree performs classification; when the response is continuous it performs regression. Starting from the root, samples are routed through successive nodes until a final class label or value is returned

Convolutional neural networks (CNNs) represent a class of artificial neural networks that are designed to process information in a manner similar to that of the human brain[32]. A distinctive feature of CNNs is their network structure, comprising multiple hidden layers, each of which contains both a convolutional layer and a pooling layer. In this study, the pre-trained convolutional neural network takes 64 × 64-pixel image patches as input. The architecture consists of 8 image-processing stages and 4 hidden layers whose neuron configurations are 9, 7, 5 and 3 units, respectively. For feature extraction, the model applies 12 feature maps to learn multi-level representations of the data. This hierarchical design captures spatially local patterns and, through successive abstraction, extracts high-level semantic features.

To test the best classification accuracy, we further design two classification experiments including Experiment A: only multi-spectral bands are used as input features and Experiment B: both multi-spectral bands and the identified 10 most important features. Due to the big UAV image size and huge work load for the entire study region, we only selected four mangrove distribution sites with intensive training and validation plots to test the effectiveness of these classification methods. The test regions include Ximen Island (Within Wenling), Wugen Town (Wenling), Taipingtang (Yuhuan) and Yanpuwan (Cangnan) (Figure 1).

2.8. Accuracy Assessment Metrics

To assess the precision of classification methods, confusion matrices were constructed based on training sample plots. The Overall Accuracy (OA), Kappa Coefficient, User's Accuracy (UA), and Producer's Accuracy (PA) were calculated based on the confusion matrices and applied to evaluate the performance of the classified land cover types. The calculation equations for OA, UA, PA and Kappa were shown below:

$$UA_i = \frac{C_{ii}}{\sum_{j=1}^{k} C_{ji}} \quad (1)$$

$$PA_i = \frac{C_{ii}}{\sum_{j=1}^{k} C_{ij}} \quad (2)$$

$$OA = \frac{\sum_{i=1}^{k} TP_i}{N} \quad (3)$$

$$Kappa = \frac{N\sum_{i=1}^{k} TP_i - \sum_{i=1}^{k}(R_i \times C_i)}{N^2 - \sum_{i=1}^{k}(R_i \times C_i)} \quad (4)$$

Where, TP_i is the number of samples correctly classified as class i, k is the total number of classes, N is the total number of samples, and P_i is the number of true samples of class i; C_i is the number of predicted samples of class i; C_{ii} denotes the number of samples correctly assigned to class i in the confusion matrix (the diagonal element for class i); C_{ji} is the number of samples for predicted class i; C_{ij} is the number of samples for true class i.

2.9. Analysis Methods

The classified mangrove and smooth cordgrass were isolated from the land cover maps. Due to the scattered distribution patterns land large size of the UAV images and classified results, we divided 11 districts and three cities (Taizhou, Wenzhou and Zhoushan; Figure 1) for mapping and statistical analysis. The direct classified results were for canopy coverage of all land cover types (Canopy area) and then they were aggregated to 30m spatial resolution for calculating area of each

 doi:10.20944/preprints202512.0901.v1

land cover types. Due to the lower height of mangrove trees in Zhejiang Province, mangrove forest area was calculated as the area with canopy coverage equal to or greater than 30%[33]. The survival rate of mangrove trees was calculated as the ratio of existing mangrove area to the total planting area. The planting area and boundary of mangroves was obtained from[33]. The invasion rate of smooth cordgrass was calculated as the ratio of existing smooth cordgrass area to the planting area of mangrove trees. The area of mangrove from previous studies was calculated after clipping the Zhejiang Province out of the national or global datasets of mangrove distribution.

3. Results

3.1. Accuracy Assessment Results

At the test regions, six categories of land cover were classified including water (WA), mangrove (MA), mudflats (MU), smooth cordgrass (SC) and built-up land (BU). Confusion matrices were constructed to calculate and compare the accuracy assessment metrics. The results indicated that the CNN method had the highest kappa coefficients of 0.96 and 0.97 and the highest overall accuracy (0.97 and 0.98) based on the all-feature and selected-feature experiments, respectively, which are significantly higher than that of DT and SVM methods for both metrics under both experiments. The selected feature experiment only slightly improved the classification accuracy using the CNN method; however, it can significantly increase the overall accuracy and kappa coefficient under DT and SVM methods. Finally, the CNN classification method was selected for the land cover classification in the study region. The classified distributions of 5 main land cover types were shown in Figure 6. Compared with the DT and SVM methods, the CNN method can more accurately detect water body and reduced the misinterpretations between mangrove trees and smooth cordgrass. Based on the CNN method, the land cover types in the entire Zhejiang were classified, and the classification results were further evaluated using 530 sampling plots. The results indicated that the overall accuracy and kappa coefficient still very high, reaching 97% and 0.96, respectively (Table 3).

Table 2. Classification accuracy assessment results at test regions.

Methods	Accuracy metrics	Experiment A (All features)	Experiment B (Selected features)
SVM	Overall Accuracy	75%	83%
	Kappa	0.63	0.76
DT	Overall Accuracy	73%	91%
	Kappa	0.62	0.88
CNN	Overall Accuracy	97%	98%
	Kappa	0.96	0.97

Table 3. Classification accuracy assessment results for the entire study region using the CNN classification methods. Note: UA: User accuracy; PA: Producer accuracy; OA: Overall accuracy; BU: Built-up land; MA: Mangroves; MU: Mudflats; SC: Smooth cordgrass; WA: Water body.

Types	SC	MA	BU	WA	MU	Samples	UA
SC	119	4	0	0	0	123	97.86%
MA	2	170	0	0	1	173	97.92%
BU	0	0	47	1	1	49	98.34%
WA	1	0	1	48	3	54	94.11%
MU	1	0	1	2	127	131	96.96%
Samples	123	174	49	51	132	530	

 doi:10.20944/preprints202512.0901.v1

PA	97.15%	98.55%	96.73%	93.74%	97.55%
OA				97.34%	
Kappa				0.96	

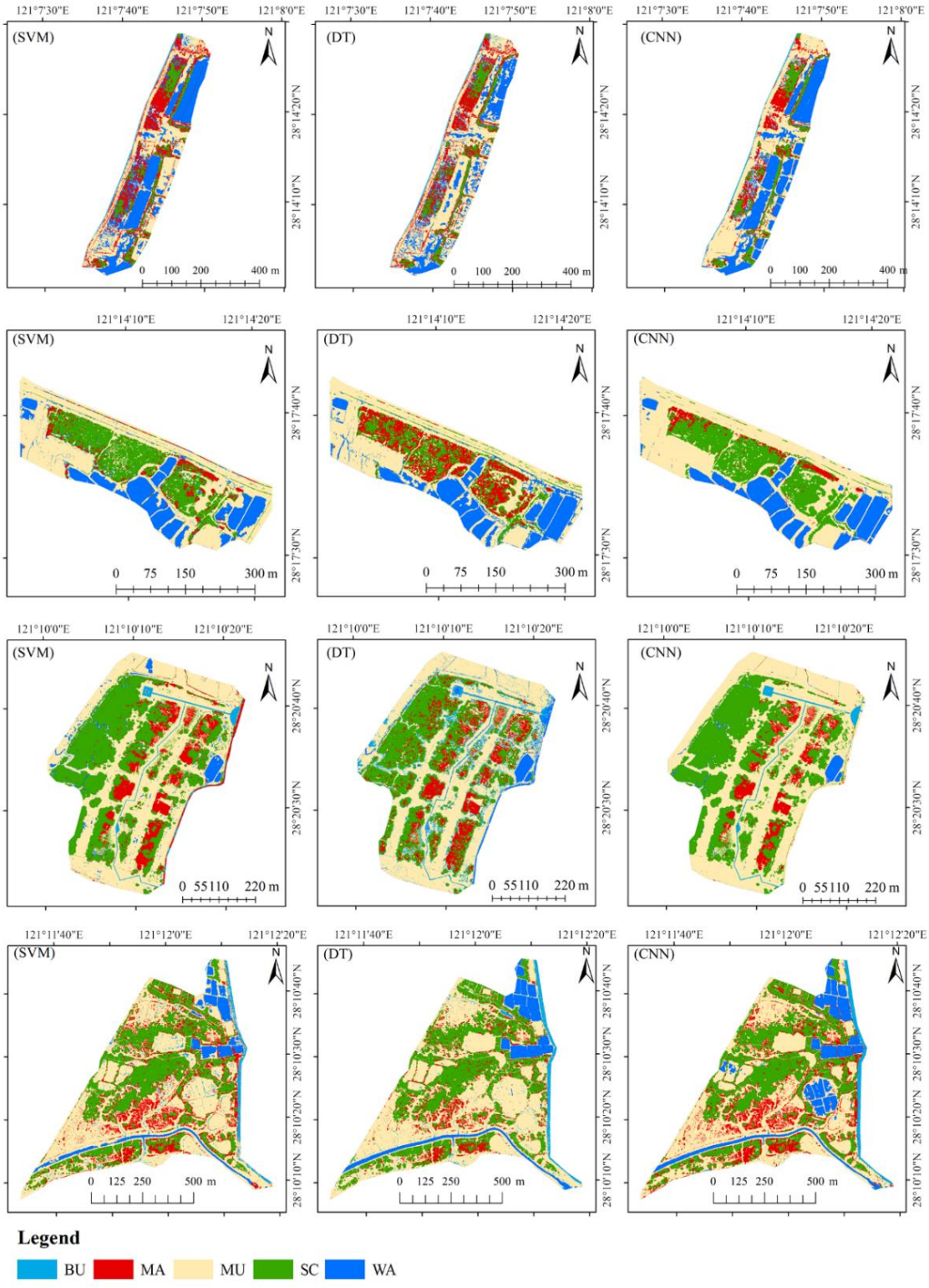

Figure 6. Classified land cover types based on different classification methods in conjunction with feature selection in four test regions. Note: Built-up land (BU), Mangroves (MA), Mudflats (MU), Smooth cordgrass (SC) and Water body (WA).

 doi:10.20944/preprints202512.0901.v1

3.2. Distribution of Mangroves and Smooth Cordgrass

Due to the higher resolution of UAV imagery, our detected area for mangroves and smooth cordgrass are actually canopy cover area. The canopy cover area of mangroves in Zhejiang Province is 115.73 ha in 2023 in Zhejiang Province, while the area of smooth cordgrass invaded in mangrove plantations is 52.95 ha (Figure 7). The total area of mangrove forests was calculated as 140.83 ha in terms of the shrub-like forest area definition (canopy coverage >= 30%) in China. At 30m pixel scale, over 70.04% of the pixels with mangrove tree distributions had canopy coverage lower than 20%, indicating that the mangrove trees are mostly distributed in a scattered manner in the planting area (Figure 8). The lower canopy density mostly distributed in the northern Zhejiang, such as Putuo, Sanmen, Jiaojiang, Wenling and Yueqing districts. The highest coverage (80-100%) only accounted for about 3.35% of the mangrove distribution area and mostly spreads in the southern Zhejiang, such as Yuhuan, Dongtou, Pingyang, Cangnan, and Longgang districts. In contrast, the highest canopy coverage (80-100%) of smooth cordgrass mostly distributed in the central and northern Zhejiang such as Jiaojiang and Wenling districts, with continuous and smaller canopy coverage in the southern Zhejiang such as Dongtou, Rui'an and Pingyang (Figure 9). Before the planting of mangrove trees, the smooth cordgrass was first mechanically removed. This resulted in its sporadically spreading pattern across the areas with mangrove tree distribution. About 81.80% the smooth cordgrass had canopy coverage lower than 20% at the 30 m spatial resolution. The smooth cordgrass distribution is more disperse than that of the mangrove trees.

At regional scale, the largest mangrove forest area is located in Dongtou district (40.92 ha), followed by Yuhuan (30.50 ha) and Yueqing (23.93 ha) districts (Figure 7). They accounted for 46%, 18.5% and 17.5% of the total mangrove area, respectively (Figure 10). Within the mangrove planting areas, the largest smooth cordgrass area is located in Yuhuan (24.35 ha), Dongtou (9.82 ha) and Yueqing (9.26 ha) districts (Figure 7). They accounted for about 29.2%, 21.0% and 16.8% of the total smooth cordgrass area (Figure 10). These three regions had both highest mangrove and smooth cordgrass area due to the habitat overlaps between both vegetation types.

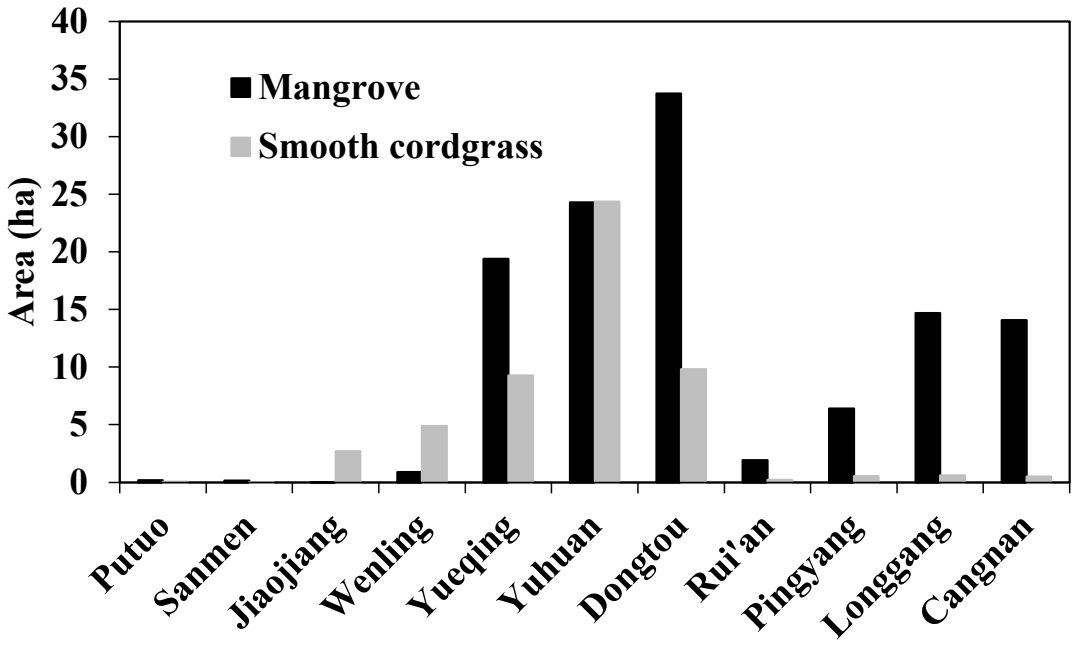

Figure 7. The area of smooth cordgrass and mangroves in the 11 districts.

 doi:10.20944/preprints202512.0901.v1

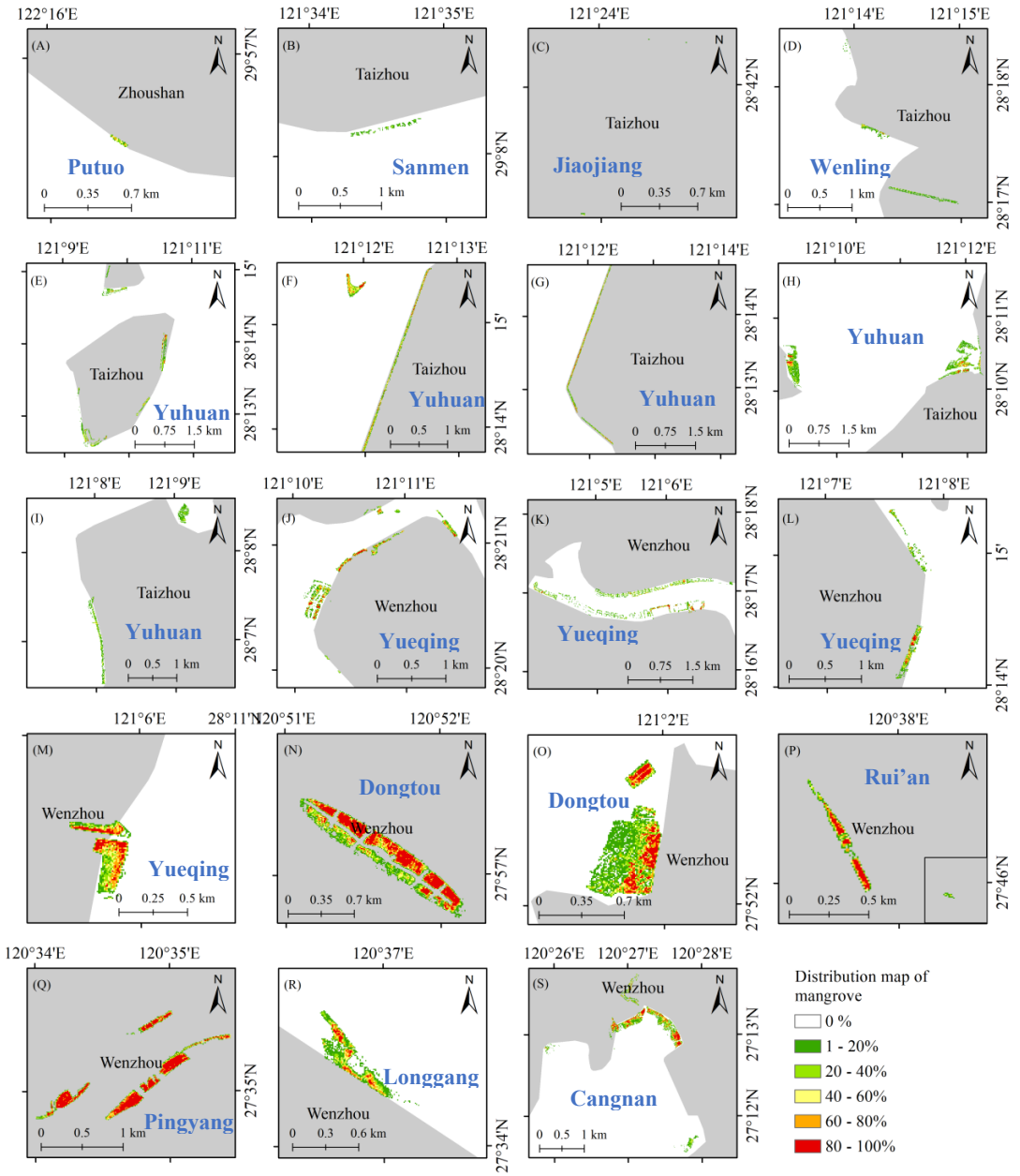

Figure 8. The canopy distribution (%) of mangroves aggregated at 30m spatial resolution in Zhejiang Province.

 doi:10.20944/preprints202512.0901.v1

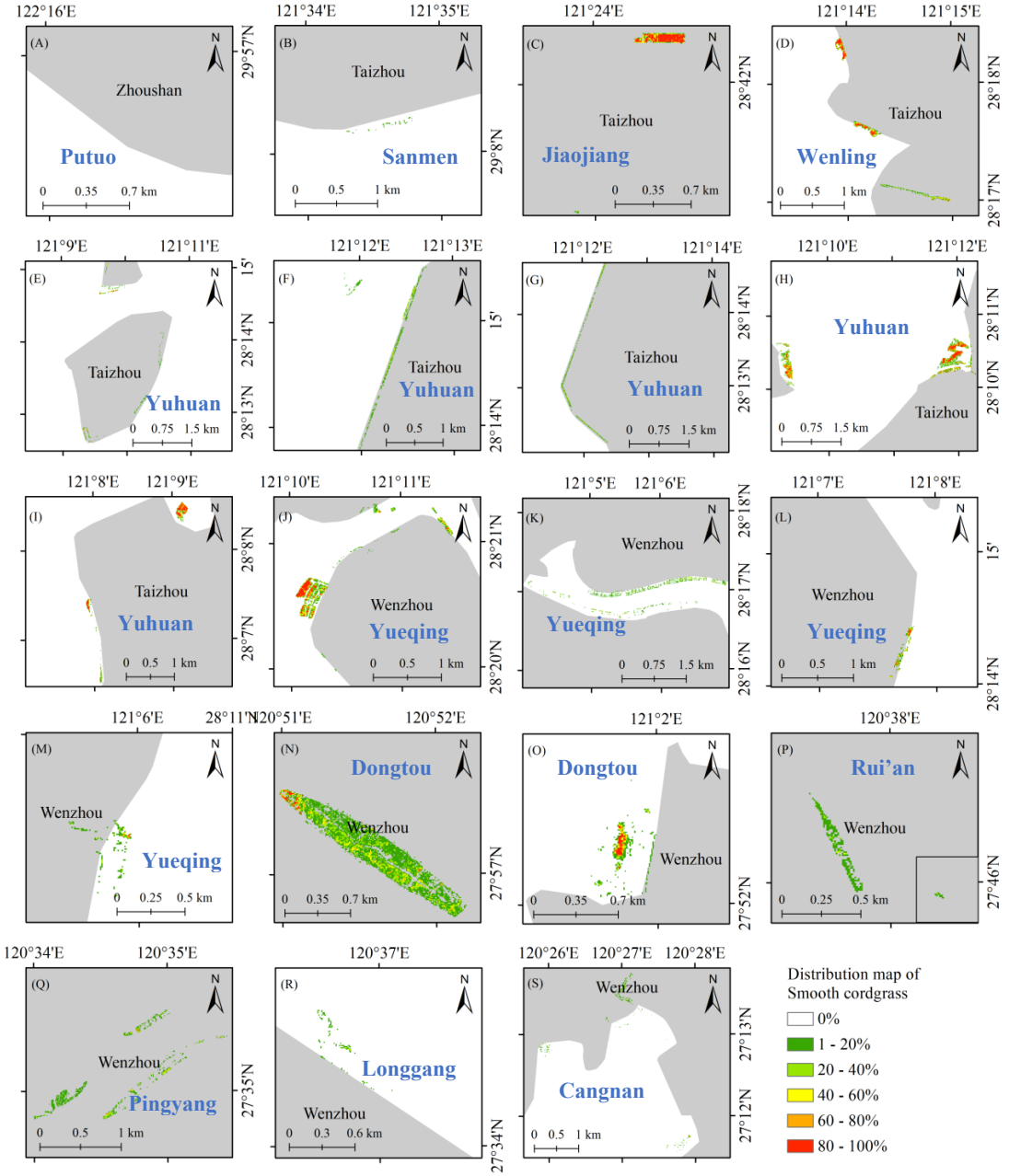

Figure 9. The distribution (%) of smooth cordgrass aggregated at 30m spatial resolution in Zhejiang Province.

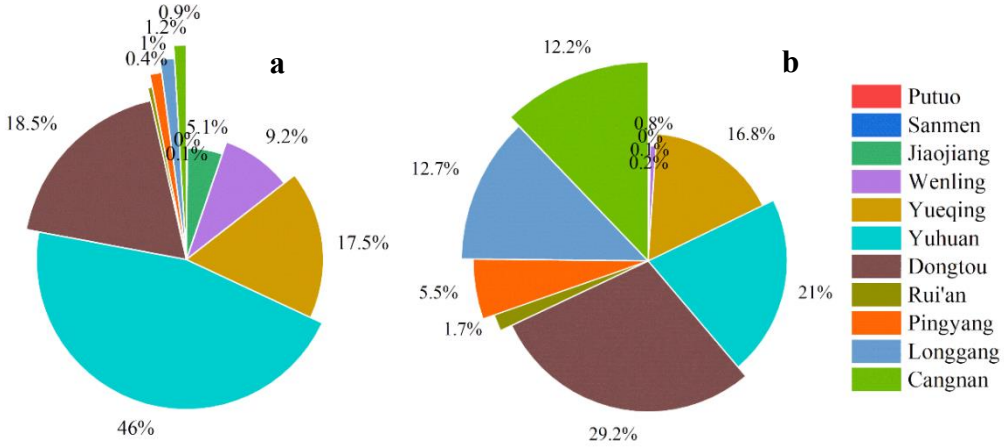

Figure 10. Percentage of smooth cordgrass (A) and mangroves (B) in each district.

 doi:10.20944/preprints202512.0901.v1

3.3. The Survival Rates of Mangrove Trees and Invasion of Smooth Cordgrass

Due to the limitation of low air temperature, strong tide and seawater submerge, invasion of smooth cordgrass and human activities, the survival rates of planted mangrove trees are very low in the study region. The current existing mangrove trees were actually replanted several times after the first planting date. Even under this condition, the survival rates were still very low (Figure 11). The reported planting area of mangrove trees were 386.77 ha; however, our study indicated that the total mangrove forest area was only 140.83 ha, showing a low survival rate of 36.41%. In other words, the mortality rate was 63.59%, which is extremely high. Among districts, the highest survival rate was shown in Rui'an (72.46%) and Pingyang (72.79%), while the lowest survival rate was shown in Jiaojiang (0.63%) and Sanmen (3.91%) districts. The survival rates in other districts ranged from 7.15% to 54.52%, with mostly lower than 50% survival rates. The survival rates generally showed a declining pattern from the south to the north of Zhejiang Province, with the lowest survival rate in the northernmost part (Figure 1). Replanting and thereafter intensive human management is definitely needed for most districts to reduce the limiting factors for mangrove tree survival.

Most mangrove trees were planted on the area after smooth cordgrass was removed. Due to its faster growth rate, taller height, and stronger competitiveness than the mangrove trees, the smooth cordgrass was invaded back soon and become one of the most important factors influencing mangrove tree survival. Our study found that about 13.7% of the mangrove planting area was occupied by smooth cordgrass. The invasion rates were extremely high in the Jiaojiang (85.44%) and Wenling (67.26%) districts, indicating that most of the planting area of mangrove trees was occupied with smooth cordgrass (Figure 11). The invasion rates of smooth cordgrass in Yueqing (19.08%) and Yuhuan (20.90%) districts were also relatively high, while the invasion rates in other districts ranged from 0.88% (Cangnan) to 9.26% (Dongtou). The area of smooth cordgrass has surpassed the mangrove area in Jiaojiang and Wenling, and is close to the mangrove area in Yuhuan. The ratio of smooth cordgrass area accounted for 99.26% and 90.39% of the total smooth cordgrass and mangrove area in Jiaojiang and Wenling, respectively. In these three districts, the invasion of smooth cordgrass could be the main cause of mangrove tree mortality.

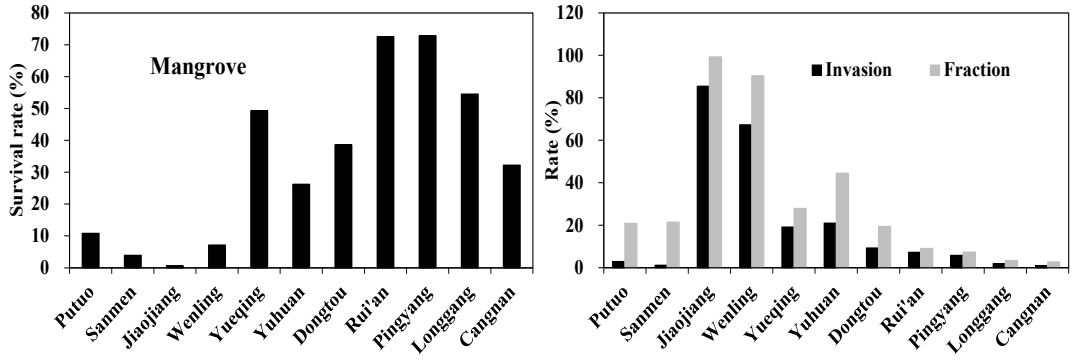

Figure 11. The survival rates of mangrove trees relative to the planting area and the invasion rates and relative fraction of smooth cordgrass. Note: the relative fraction is calculated as the ratio of smooth cordgrass to the total area of smooth cordgrass and mangrove trees.

The different levels of mangrove survival rates and smooth cordgrass invasion rates were also illustrated in Figure 12. Generally, two types of invasion patterns of smooth cordgrass were observed. The first type is spreading in the open gaps after the mangrove trees die, and the second type is spreading from the periphery to the central distribution area of mangrove trees. The first type is mainly occurred in the southern Zhejiang, while the second type is more popular in the farther northern Zhejiang. This resulted in the highest coverage of smooth cordgrass in the northern districts.

 doi:10.20944/preprints202512.0901.v1

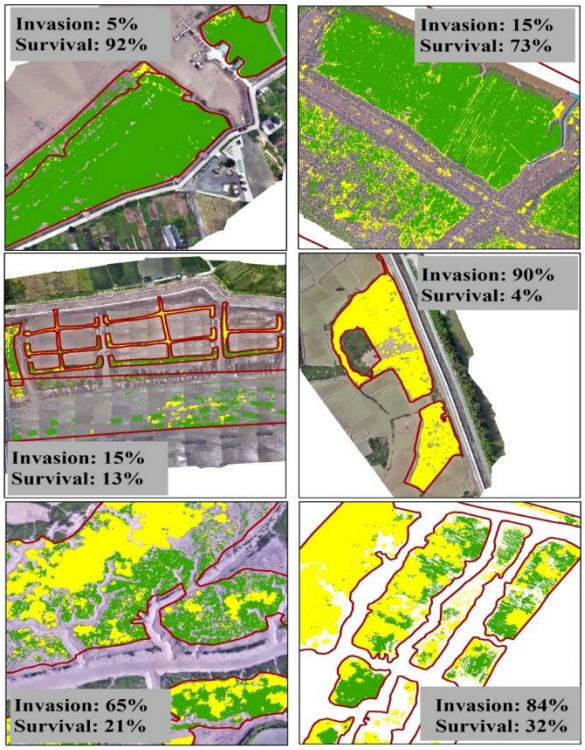

Figure 12. The illustration of invasion rate of smooth cordgrass and survival rate of mangrove trees in six selected areas. Note: The background map is the UAV RGB images. The map scale is at 1:4,000.

4. Discussion

4.1. The Mangrove Area in Zhejiang Province

The reported planted area of the mangrove trees was 386.77 ha in 2022[33]. But from our study, the actual survival area of mangrove forests was only 140.83 ha, with a survival rate of 36.41%. Among the mangrove forest area, only about 33.30 ha was reported as closed canopy[15], also indicating a low survival rate in this study region. The high mortality rate was mainly attributed to the cold stress, sheltering by smooth cordgrass, seawater submerge, and insects & diseases[15,33,34]. Based on the land cover classification results (Figure 6), we observed that most of the mangrove area was replaced by mudflat (bare mud), water body and the smooth cordgrass.

Many previous studies have also estimated the mangrove area in Zhejiang Province, showing a range from 6.12 ha to 386.77 ha during 2015-2020, with a median area of 47 ha (Table 4). For example, in the Global Mangrove Watch (GMW) dataset, the mangrove forest area in 2020 was 47 ha based on the classification from ALOS SAR imagery[3]; Hu et al. [35] estimated that only 6.12 ha existed in 2015; Wu et al.[33] reported the largest area of 386.77 ha, mainly because they identified the planting area of mangrove trees rather than the canopy cover area. This large discrepancy is mainly due to the difference in report time, remote sensing tools and classification methods. Due to the lower canopy coverage, lower tree height and compounding effects from smooth cordgrass, the middle (e.g., Sentinel, Landsat and ALOS) resolution satellite images are not able to effectively capture the mangrove reflectance information[21,34]. Zhao and Qin [21] and Zhang et al. [20] have also explained the large gaps among different studies for mangrove area and attributed to the compounding effects of other coastal vegetation types, especially the smooth cordgrass. The mangrove trees are relatively short and of a similar height to smooth cordgrass, which makes them difficult to distinguish[31]. In addition, the observation time period also significantly affects the estimated mangrove area because the planting area in Zhejiang Province was increasing rapidly especially in the recent decade[15,33]. The 52.06% mangrove forests are younger than 3 years' old in Zhejiang Province[33]. The small plants

 doi:10.20944/preprints202512.0901.v1

and low canopy density could result in a very low classification accuracy using the middle resolution and relatively high resolution imagery[13,20].

Based on the high resolution UAV multispectral imagery, the identified best classification method and extensive field inventory data, our approach can more effectively differentiate the mangrove trees from the smooth cordgrass and provides a more robust and updated mangrove area data for Zhejiang Province.

Table 4. The comparison of our estimated mangrove forest area with previous studies for Zhejiang Province.

Platforms	Time	Area (ha)	Resolution	References
ALOS SAR image	2020	47	23.5m	[3]
Landsat and Sentinel-1	2015	8.0	30m	[36]
Landsat image	2015	56	30m	[5]
Landsat image	2015	6.12	30m	[35]
Gaofen-1 and Ziyuan-3	2018	48.68	2m	[20]
Sentinel-1 & 2	2019	39	20m	[21]
Statistical and inventory	2020	386.77	/	[33]
UAV multispectral image	2023	140.83	4 & 6 cm	This study

4.2. The Invasion Patterns of Smooth Cordgrass

The invasion of smooth cordgrass into mangrove forests has been reported worldwide[9]. The smooth cordgrass expansion can directly affect mariculture activities and shorebirds that forage on the mudflat[15,37]. In addition, its high density, strong root system and tall height can significantly affect the growth rate of mangrove trees and result in high mortality[18]. Most mangrove trees in Zhejiang Province were planted on the smooth cordgrass habitats after removing all smooth cordgrass because these areas were also proved to be suitable for mangrove tree species *K. obovata[15,25]*. In addition, the smooth cordgrass has been recognized as an invasive species by China's Ministry of Ecology and Environment in 2003, and the government was encouraged to control its spreading. Our study indicated that 52.95 ha of smooth cordgrass exist in the mangrove planting area at present, accounting for about 13.7% of the total planting area. This is under condition of frequent mechanical and chemical controls within the first several years after mangrove trees were planted[33]. But the control measures can not guarantee the prevention of the expansion of smooth cordgrass[15]. We also found that the smooth cordgrass invasion was more severe in the central Zhejiang Province rather than the northern region where the mangrove tree size is shorter and smaller. For example, the densest smooth cordgrass coverage (80-100%) was mainly shown in the central area (Figure 9), and Jiaojiang, Wenling and Yuhuan districts have the highest coverage (greater than 20%) (Figure 11). This can be explained by that the lower temperature in the north is not too suitable for smooth cordgrass to invasion, while the higher temperature and small size of mangrove trees in the central can not prevent its sprouting and invasion. Certainly, the most suitable habitats are in the southern Zhejiang such as Longgang, Cangnan, and Pingyang districts, but the mangrove trees in this area have become dense forests with closed canopy. The denser coverage and height of mangrove trees prevented the invasion of smooth cordgrass[13].

4.3. Implications for Mangrove Management and Smooth Cordgrass Control

The mangrove forests along the coastlines have important functions in beach fixation and wave reduction, soil nutrient cycling, hydrological regulation, air purification, carbon sequestration, and biodiversity conservation[3,8,9]. To protect and restore mangrove forests, many countries or organizations are on action by implementing protection plans, policies or regulations. Such actions will support coastal communities, jobs and food security, and provide global climate mitigation

 doi:10.20944/preprints202512.0901.v1

benefits [8]. For example, Global Mangrove Alliance (GMA) was established in 2021 to convene the worldwide governments or organizations to protect mangrove resources. The Chinese government has also released the "Special Action Plan for Mangrove Conservation and Restoration (2020-2025)" in 2020[33]. Under this plan, Zhejiang Province needs to expand mangrove forest area to 690 ha[15]; however, the current existing mangrove forest area is only 140.83 ha, which is far away from the targeted area. Therefore, to scientifically guide the protection and restoration efforts in Zhejiang Province, it is necessary to identify the exact distribution information and the causes of area losses of mangrove forests. Our study provides a more accurate monitoring of the mangrove distribution area, which will help guide the replanting and management planning activities, and accurate estimation of carbon stock for mangrove forests.

The survival rates of mangrove trees were extremely low in Zhejiang Province, especially in Jiaojiang, Wenling and Yuhuan districts, with mangrove tree coverage mostly lower than 20%. Replanting of mangrove trees is definitely needed. In addition, the major causes of mortality should be identified to avoid damages on planted mangrove trees. Smooth cordgrass invasion is one of the most important causes. Our study clarified the distribution and coverage of smooth cordgrass, which will help the local decision makers or managers to control the spreading of smooth cordgrass in mangrove forests in Zhejiang Province. The canopy density of mangrove trees has been reported to significantly affect the invasion rates of smooth cordgrass[13,38]. Kan et al. [13] indicated that 41-64% canopy coverage of mangrove trees could significantly suppress the invasion of smooth cordgrass and >65% coverage could completely suppress in Fujian Province. We also observed a large decline of smooth cordgrass coverage when mangrove canopy coverage was greater than 40%. Therefore, at the districts with mangrove coverage over 40%, anthropogenic intervention is not necessary to conduct, such as Longgang (45.45%), Rui'an (62.80%) and Pingyang (68.36%) districts. In contrast, removal of smooth cordgrass is needed in the districts with extremely low mangrove canopy coverage and high invasion rates. For example, Jiaojiang, Wenling and Yuhuan districts have mangrove coverage of 0.38%, 12.31%, and 20.83%, respectively but invasion rates of 85.44%, 67.26% and 20.90% respectively. Anthropogenic control measures are urgently needed in these three districts to protect mangrove trees.

4.4. Limitations and Future Direction

Although our classifications using the UAV image and machine learning methods achieved a high precision, there are several limitations that may compound our results and conclusion. Due to the similar reflectance characteristics between mangrove trees and smooth cordgrass, taller height of smooth cordgrass, and the small size and shorter height of mangrove trees, some mangrove trees are sheltered by the smooth cordgrass plants and are not able to be recognized by our methods. UAV images in non-growing seasons are needed to assist classifying this under-covered mangrove trees since their growth because smooth cordgrass is a deciduous species and mangrove tree is an evergreen species. In addition, the training and validation plots from survey and visual interpretation were obtained at 5 m×5 m grid scale, which may not match well with the segmented polygons in both area and shape, which will also bring classification errors. Finally, we only used one-period UAV imagery to analyze the distribution of mangrove trees and invasion status of smooth cordgrass. The temporal variations can not be addressed through our UAV approach, thus we can not analyze the effects of smooth cordgrass invasion on the mortality of mangrove trees. In the future, we will apply multi-temporal UAV based multispectral and LiDAR images to monitor the dynamics of mangrove trees and smooth cordgrass and to estimate mangrove biomass and carbon sequestration in Zhejiang Province.

5. Conclusions

Based on provincial scale multispectral UAV imagery, this study screened the most important features to differentiate the mangrove trees from smooth cordgrass and identified the optimal segmentation scale parameters. Four object-based classification methods were compared in the test

 doi:10.20944/preprints202512.0901.v1

regions and the best method of CNN was identified. The land cover types within the planting area of mangrove trees were then detected using the CNN method. The results indicated that only 140.83 ha mangrove forests out of 386.77 ha planting area were survived in Zhejiang Province, suggesting a high mortality rate. The invasion of smooth cordgrass was one of the most important causes of the high mortality rate of mangrove trees. The survival rates in some planting districts were lower than 10%, implying an urgent need to replant mangrove trees to restore mangrove forest area. The smooth cordgrass was expanded to 52.96 ha and its area has surpassed the mangroves in some districts in the central and northern Zhejiang Province, suggesting anthropogenic intervention is needed to remove or reduce the smooth cordgrass. Smooth cordgrass invasion can be suppressed when the mangrove canopy coverage is greater than 40%, which means that anthropogenic intervention is urgently needed for those mangrove planting area with low canopy coverage. Our study provides an accurate inventory of mangrove forest area and the distribution of smooth cordgrass, which will help guide the local agencies to protect mangrove forests, and remove or control the spreading of smooth cordgrass. Our results will also provide data basis for the future planning of mangrove planting and the estimation of carbon stock capacity and potential in mangrove forests.

Author Contributions: Conceptualization, G.C.; methodology, Q.L.; software, Q.L.; validation, Q.L. and S.Y.; formal analysis, Q.L., P.Z. and J.Y.; investigation, Q.L., P.Z. and Y.S.; resources, X.X.; data curation, Q.L., P.Z., S.Y., Y.S. and J.Y.; writing—original draft preparation, Q.L.; writing—review and editing, Y.S., J.M. and G.C.; visualization, Q.L., P.Z., J.Y. and G.C.; supervision, G.C.; project administration, S.Y. and Y.S.; funding acquisition, J.M. and G.C. All authors have read and agreed to the published version of the manuscript.

Funding: Please add: This research was funded by the Key Research and Development Program of Zhejiang Province (Grant number 2023C02003), Wenzhou High-level Innovation Team "Coastal Characteristic Plant Innovation and Utilization Project" (Grant number NY202401) and the foundation for Key Laboratory of Ecology of Rare and Endangered Species and Environmental Protection, Ministry of Education (Grant number ERESEP2025K02).

Data Availability Statement: All data generated or analyzed during this study are included in this article.

Acknowledgments: We thank the assistances of Jiahua Chen and other students involving in the field survey and data analysis during this study.

Conflicts of Interest: The authors declare no conflicts of interest.

References

1. Giri, C.; Ochieng, E.; Tieszen, L.L.; Zhu, Z.; Singh, A.; Loveland, T.; Masek, J.; Duke, N. Status and distribution of mangrove forests of the world using earth observation satellite data. *Global Ecology and Biogeography* **2011**, *20*, 154-159.
2. Wang, Y.; Dong, P.; Hu, W.; Chen, G.; Zhang, D.; Chen, B.; Lei, G. Modeling the Climate Suitability of Northernmost Mangroves in China under Climate Change Scenarios. *Forests* **2022**, *13*, 64.
3. Bunting, P.; Rosenqvist, A.; Hilarides, L.; Lucas, R.M.; Thomas, N.; Tadono, T.; Worthington, T.A.; Spalding, M.; Murray, N.J.; Rebelo, L.-M., *et al.* Global mangrove extent change 1996–2020: Global Mangrove Watch Version 3.0. *Remote Sensing* **2022**, *14*, 3657.
4. Goldberg, L.; Lagomasino, D.; Thomas, N.; Fatoyinbo, T. Global declines in human-driven mangrove loss. *Global Change Biology* **2020**, *26*, 5844-5855.
5. Jia, M.; Wang, Z.; Zhang, Y.; Mao, D.; Wang, C. Monitoring loss and recovery of mangrove forests during 42 years: The achievements of mangrove conservation in China. *International journal of applied earth observation and geoinformation* **2018**, *73*, 535-545.
6. Jia, M.; Wang, Z.; Li, L.; Song, K.; Ren, C.; Liu, B.; Mao, D. Mapping China's mangroves based on an object-oriented classification of Landsat imagery. *Wetlands* **2014**, *34*, 277-283.

 doi:10.20944/preprints202512.0901.v1

7. Massey, R.; Berner, L.T.; Foster, A.C.; Goetz, S.J.; Vepakomma, U. Remote Sensing Tools for Monitoring Forests and Tracking Their Dynamics. In *Advances in Global Change Research*, Springer Science and Business Media B.V.: 2023; pp 637-655.
8. Romañach, S.S.; DeAngelis, D.L.; Koh, H.L.; Li, Y.; Teh, S.Y.; Raja Barizan, R.S.; Zhai, L. Conservation and restoration of mangroves: Global status, perspectives, and prognosis. *Ocean & Coastal Management* **2018**, *154*, 72-82.
9. Biswas, S.R.; Biswas, P.L.; Limon, S.H.; Yan, E.-R.; Xu, M.-S.; Khan, M.S.I. Plant invasion in mangrove forests worldwide. *Forest Ecology and Management* **2018**, *429*, 480-492.
10. Zhang, X.; Zhang, Z.; Li, Z.; Li, M.; Jiang, M. Impacts of Spartina alterniflora invasion on soil carbon contents and stability in the Yellow River Delta, China. *Science of The Total Environment* **2021**, *775*, 145188.
11. Wu, M. Spatial distribution and influencing factors of the biomass of Spartina Alterniflora in coastal wetlands of Zhejiang. Chinese Academy of Forestry, Beijing, China, 2018.
12. Zhou, Z.; Yang, Y.; Chen, B. Estimating the Spartina alterniflora fractional vegetation cover using high spatial resolution remote sensing in a coastal wetland. *Acta Ecologica Sinica* **2017**, *37*, 505-512.
13. Kan, Z.; Chen, B.; Yu, W.; Shunyang, C.; Chen, G. Risk identification of mangroves facing Spartina alterniflora invasion using data-driven approaches with UAV and machine learning models. *Remote Sensing of Environment* **2025**, *319*, 114613.
14. Chen, B.; Xiao, X.; Li, X.; Pan, L.; Doughty, R.; Ma, J.; Dong, J.; Qin, Y.; Zhao, B.; Wu, Z., *et al.* A mangrove forest map of China in 2015: Analysis of time series Landsat 7/8 and Sentinel-1A imagery in Google Earth Engine cloud computing platform. *ISPRS Journal of Photogrammetry and Remote Sensing* **2017**, *131*, 104-120.
15. Chen, Q.; Yang, S.; Wang, J.; Liu, X.; Zheng, J.; Deng, R. Development history and discussion of mangrove forest in Zhejiang Province. *Journal of Zhejiang Agricultural Sciences* **2019**, *60*, 1177-1181.
16. Li, L.; Mao, D.; Wang, Z.; Huang, X.; Li, L.; Jia, M. Diffusion dynamics and driving forces of Spartina alterniflora in the Guangxi Shankou Mangrove Reserve. *Acta Ecologica Sinica* **2021**, *41*, 6814-6824.
17. Wu, K.X.; Gao, G.; Zhao, Y.; Zhang, Y.; Wu, Y.; Yang, N.; Yu, Q.; Lin, J.; Lu, C. Monitoring and Analysis of Driving Factors in the Mangrove-Salt Marsh Intertidal Zone Changes at Zhangjiang Estuary. *Journal of Chifeng University (Natural Science Edition)* **2024**, *40*, 1-7.
18. Zhang, Y.; Huang, G.; Wang, W.; Chen, L.; Lin, G. Interactions between mangroves and exotic Spartina in an anthropogenically disturbed estuary in southern China. *Ecology* **2012**, *93*, 588-597.
19. Kuenzer, C.; Bluemel, A.; Gebhardt, S.; Quoc, T.V.; Dech, S.; Kuenzer, C.; Bluemel, A.; Gebhardt, S.; Quoc, T.V.; Dech, S. Remote sensing of mangrove ecosystems: a review. *Remote Sensing* **2011**, *3*, 878-928.
20. Zhang, T.; Hu, S.; He, Y.; You, S.; Yang, X.; Gan, Y.; Liu, A.; Zhang, T.; Hu, S.; He, Y., *et al.* A fine-scale mangrove map of China derived from 2-meter resolution satellite observations and field data. *ISPRS International Journal of Geo-Information* **2021**, *10*, 92.
21. Zhao, C.; Qin, C. A detailed mangrove map of China for 2019 derived from Sentinel-1 and -2 images and Google Earth images. *Geoscience Data Journal* **2022**, *9*, 74-88.
22. Pan, W.; Chen, J.; Wang, Y. Analysis of spatio-temporal dynamical change and landscape characteristics of mangroves and Spartina alterniflora in Fujian based on satellite imageries from 1999 to 201. *Journal of Ecology and Rural Environment* **2020**, *36*, 1428-1436.
23. Yang, Y.; Meng, Z.; Zu, J.; Cai, W.; Wang, J.; Su, H.; Yang, J.; Yang, Y.; Meng, Z.; Zu, J., *et al.* Fine-scale mangrove species classification based on UAV multispectral and hyperspectral remote sensing using machine learning. *Remote Sensing* **2024**, *16*, 3093.
24. Liu, M.; Li, H.; Li, L.; Man, W.; Jia, M.; Wang, Z.; Lu, C.; Liu, M.; Li, H.; Li, L., *et al.* Monitoring the invasion of Spartina alterniflora using multi-source high-resolution imagery in the Zhangjiang Estuary, China. *Remote Sensing* **2017**, *9*, 539.
25. Lu, X.; Liu, X.; Wang, J.; Yang, S.; Zhang, L.; Ji, H.; Chen, Q. Study on overwintering methods for introduced Kandelia obovata in Jiangsu Province. *Forestry Science & Technology* **2019**, *44*, 15-17.
26. Kursa, M.B.; Rudnicki, W.R. Feature selection with the Boruta package. *Journal of Statistical Software* **2010**, *36*, 1-13.
27. Azzeh, J.; Zahran, B.; Alqadi, Z. Salt and Pepper Noise: Effects and Removal. *JOIV: International Journal on Informatics Visualization* **2018**, *2*, 252-256.

 doi:10.20944/preprints202512.0901.v1

28. Heumann, B.W. An Object-Based Classification of Mangroves Using a Hybrid Decision Tree—Support Vector Machine Approach. *Remote Sensing* **2011**, *3*, 2440-2460.
29. Arfan, A.; Nyompa, S.; Maru, R.; Nurdin, S.; Juanda, M.F. Mapping Analysis of Mangrove Areas using Unmanned Aerial Vehicle (UAV) Method in Maros District South Sulawesi. *Journal of Physics: Conference Series* **2021**, *2123*, 012010.
30. Wang, D.; Wan, B.; Qiu, P.; Su, Y.; Guo, Q.; Wu, X. Artificial mangrove species mapping using Pléiades-1: an evaluation of pixel-based and object-based classifications with selected machine learning algorithms. *Remote Sensing* **2018**, *10*, 294.
31. Lewis, R.R.; Milbrandt, E.C.; Brown, B.; Krauss, K.W.; Rovai, A.S.; Beever, J.W.; Flynn, L.L. Stress in mangrove forests: Early detection and preemptive rehabilitation are essential for future successful worldwide mangrove forest management. *Marine Pollution Bulletin* **2016**, *109*, 764-771.
32. Osco, L.P.; Marcato Junior, J.; Marques Ramos, A.P.; De Castro Jorge, L.A.; Fatholahi, S.N.; De Andrade Silva, J.; Matsubara, E.T.; Pistori, H.; Gonçalves, W.N.; Li, J. A review on deep learning in UAV remote sensing. *International Journal of Applied Earth Observation and Geoinformation* **2021**, *102*, 102456.
33. Wu, W.; Zhao, Z.; Yang, S.; Liang, L.; Chen, Q.; Lu, X.; Liu, X.; Zhang, X. The mangrove forest distribution and analysis of afforestation effect in Zhejiang Province. *Journal of Tropical Oceanography* **2022**, *41*, 67-74.
34. Wang, L.; Jia, M.; Yin, D.; Tian, J. A review of remote sensing for mangrove forests: 1956-2018. *Remote Sensing of Environment* **2019**, *231*, 111223.
35. Hu, L.; Li, W.; Xu, B. Monitoring mangrove forest change in China from 1990 to 2015 using Landsat-derived spectral-temporal variability metrics. *International Journal of Applied Earth Observation and Geoinformation* **2018**, *73*, 88-98.
36. Chen, B.; Xiao, X.; Li, X.; Pan, L.; Doughty, R.; Ma, J.; Dong, J.; Qin, Y.; Zhao, B.; Wu, Z. A mangrove forest map of China in 2015: Analysis of time series Landsat 7/8 and Sentinel-1A imagery in Google Earth Engine cloud computing platform. *ISPRS Journal of Photogrammetry and Remote Sensing* **2017**, *131*, 104-120.
37. Tian, J.; Wang, L.; Li, X.; Gong, H.; Shi, C.; Zhong, R.; Liu, X. Comparison of UAV and WorldView-2 imagery for mapping leaf area index of mangrove forest. *International Journal of Applied Earth Observation and Geoinformation* **2017**.
38. Jiang, Y.; Zhang, L.; Yan, M.; Qi, J.; Fu, T.; Fan, S.; Chen, B.; Jiang, Y.; Zhang, L.; Yan, M., *et al.* High-resolution Mangrove forests classification with machine learning using Worldview and UAV hyperspectral data. *Remote Sensing* **2021**, *13*, 1529.